

GALERKIN LEAST-SQUARES APPROXIMATION FOR VISCOPLASTIC FLOWS THROUGH AN ABRUPT EXPANSION

Filipe Silveira, fsilveira@mecanica.ufrgs.br; Sérgio Frey, frey@mecanica.ufrgs.br

Laboratory of Computational and Applied Fluid Mechanics (LAMAC), Mechanical Engineering Department, Universidade Federal do Rio Grande do Sul

Flávia Zinani, fszinan@ucs.br

Mechanical Engineering Department, Universidade de Caxias do Sul, Caxias do Sul, RS

Maria Laura Martins-Costa, laura@mec.uff.br

Laboratory of Theoretical and Applied Mechanics (LMTA), Mechanical Engineering Department – PGMEC, Universidade Federal Fluminense

Abstract. Bingham constitutive model characterizes the behavior of many industrial fluids presenting a yield stress limit. In this article the classical Bingham model was regularized by the equation proposed by Papanastasiou, in order to investigate the unyielded zones morphology of viscoplastic materials flowing through a planar sudden expansion. The employed mechanical model consists of the viscoplastic constitutive hypothesis coupled with continuity and motion equations. This model was approximated by a Galerkin least-squares methodology to enhance the classical Galerkin stability without upsetting its consistency. Numerical simulations of 4:1 sudden expansion flows, employing usual Lagrangian bilinear interpolations, have been performed for values of the Bingham number from $Bn=3.9$ to $Bn=127$ and Reynolds number from $Re=1$ to $Re=30$, in order to take into account yield stress and inertial effects. The numerical simulations allowed the computation of material yielded surfaces, pressure drops and velocity profiles through the expansion channel.

Keywords: Non-Newtonian fluids; Regularized Bingham model; Papanastasiou equation, Galerkin least-squares method.

1. INTRODUCTION

Bingham constitutive model was built to describe the behavior of linear viscoplastic materials such as cements, drilling muds, tomato sauce and toothpaste (Bird *et al.*, 1983). However, this model suffers from the shortcoming of describing yielded and unyielded regions by distinct equations. Papanastasiou (1987) proposed a regularization to describe the whole shear stress domain by a single equation. This work aims at performing mixed Galerkin least-squares approximations for linear viscoplastic fluid flows through a 4:1 planar sudden expansion using the Bingham model regularized by Papanastasiou equation as well as investigating how the yield stress and inertia effects affect the morphology of the yield surface and the flow dynamics. The difficulties inherent to the classical Galerkin method in inelastic non-Newtonian fluids are the compatibility between the finite element subspaces for velocity and pressure (the well-known Babuška-Brezzi condition), the difficulty to hand with geometrical non-linearity - due to the asymmetric features of advective term of motion equation - and material non-linearity – concerning the shear-thinning effects and materials subjected to yield limit.

In this article a mixed Galerkin least-squares (GLS) methodology was employed in order to circumvent Babuška-Brezzi condition (see Babuška, 1973 and Brezzi, 1974) admitting any combination between velocity and pressure finite subspaces, and to hold stability even in advective dominated zones. The GLS formulation is devoid of spurious oscillations which pollute the Galerkin approximations for velocity and pressure fields of high advective-diffusive flows (Franca and Frey, 1992). The GLS method is built in by adding to the classical Galerkin formulation mesh-dependent terms – functions of the residual of the Euler-Lagrange equation – enhancing the formulation stability without upsetting its consistency, since the exact solution trivially satisfies the residual of the Euler-Lagrange equation. In this work the GLS methodology is employed to approximate regularized Bingham fluid flows, investigating the yielded and unyielded zones morphology in flows through a planar sudden expansion, for distinct values of Bingham and Reynolds numbers.

2. MECHANICAL MODEL

The mechanical model employs the continuity and motion equations for the steady-state isothermal flows of inelastic incompressible fluids:

$$\begin{aligned} \operatorname{div} \mathbf{u} &= 0 \\ \rho [\nabla \cdot \mathbf{u}] \mathbf{u} &= \operatorname{div} \mathbf{T} + \mathbf{f} \end{aligned} \quad (1)$$

where \mathbf{u} represents the fluid velocity, ρ its mass density, \mathbf{f} the body force per unit mass and \mathbf{T} the Cauchy stress tensor.

The generalized Newtonian constitutive equation (GNL) was assumed to relate the internal stresses to kinematic variables:

$$\mathbf{T} = -p\mathbf{I} + \boldsymbol{\tau} = -p\mathbf{I} + 2\eta(\dot{\gamma})\mathbf{D}(\mathbf{u}) \quad (2)$$

where p is a mean pressure, $p \equiv -1/3\text{tr}(\mathbf{T})$, \mathbf{I} the unit tensor, $\boldsymbol{\tau}$ the viscous stress tensor and $\mathbf{D}(\mathbf{u})$ is the rate of strain tensor, whose magnitude is given by $\dot{\gamma} = (2\text{tr}\mathbf{D}^2)^{1/2}$. Besides, $\eta(\dot{\gamma}) \equiv \tau/\dot{\gamma}$ is the GNL viscosity function, (Bird et al, 1983).

In order to model the stress-strain behavior of a viscoplastic material we have chosen Bingham constitutive model. This model is characterized by a linear viscoplastic relation between shear stress and shear rate, flowing like a Newtonian fluid when the shear stress of the material exceeds its yield value τ_0 . For shear stress values below τ_0 , moving or unmoving (dead) unyielded zones are characterized. This model is expressed by (Bird et al., 1983):

$$\begin{aligned} \tau &= \tau_0 + \eta_0 \dot{\gamma} & \text{for } \tau \geq \tau_0 \\ \dot{\gamma} &= 0 & \text{for } \tau < \tau_0 \end{aligned} \quad (3)$$

where $\tau = (1/2\text{tr}\boldsymbol{\tau}^2)^{1/2}$ represents the shear stress magnitude, η_0 a constant Newtonian viscosity and τ_0 and $\dot{\gamma}$ have been previously defined (Bird et al., 1983).

Papanastasiou (1987) proposed a modification of Eq. (3) by introducing a regularization parameter m , which expresses the shear stress as continuous function, valid for the whole shear rate domain, eliminating the discontinuity on the τ field. The resulting regularized equation is valid for both yielded and unyielded zones, giving rise to the following shear stress and viscosity functions:

$$\tau = \eta_0 \dot{\gamma} + \tau_0 [1 - \exp(-m\dot{\gamma})] \quad ; \quad \eta(\dot{\gamma}) = \eta_0 + \frac{\tau_0}{\dot{\gamma}} [1 - \exp(-m\dot{\gamma})] \quad (4)$$

Eq. (4) states that as $m \rightarrow 0$, $\tau(\dot{\gamma})$ reduces to the classical Newtonian model and, consequently, $\eta(\dot{\gamma})$ tends to the Newtonian constant viscosity and as $m \rightarrow \infty$, $\tau(\dot{\gamma})$ becomes the classical Bingham equation and $\eta(\dot{\gamma})$ tends to the Bingham viscosity function.

3. NUMERICAL APPROXIMATION

Taking the mass and momentum balance equations, Eq.(1), for an inelastic incompressible fluid on steady-state flow, coupled with the regularized Bingham constitutive model, Eq.(4), we have the following boundary value problem:

$$\begin{aligned} \rho[\nabla \cdot \mathbf{u}] - \text{div}[2\eta(\dot{\gamma})\mathbf{D}(\mathbf{u})] + \nabla p &= \mathbf{f} & \text{in } \Omega \\ \text{div } \mathbf{u} &= 0 & \text{in } \Omega \\ \mathbf{u} &= \mathbf{u}_g & \text{on } \Gamma_g \\ [-p\mathbf{I} + 2\eta(\dot{\gamma})\mathbf{D}(\mathbf{u})]\mathbf{n} &= \mathbf{t}_h & \text{on } \Gamma_h \end{aligned} \quad (5)$$

where Ω represents the internal domain, Γ_g the portion of the boundary Γ on which Dirichlet condition is imposed and Γ_h the portion of the boundary Γ on which Neumann condition is imposed. Also, \mathbf{u}_g is the prescribed velocity field, \mathbf{t}_h the stress vector on Γ_h and $\eta(\dot{\gamma})$ is the regularized viscosity function – given by Eq. (4). The remaining variables have been previously defined.

The finite element method is built in by employing an conforming approximation – namely an approximation of spaces with infinite dimension through convenient discrete subspaces, in which, if $\mathbf{V}^h \subset \mathbf{V}$ and $P^h \subset P$, in finite dimension it comes that the finite element approximation for velocity and pressure fields are given by:

$$\begin{aligned} \mathbf{u}^h(\mathbf{x}) &= \sum_{j=1}^N u_j^h(\mathbf{x}) \mathbf{e}_j \quad ; \quad \mathbf{u}_j^h(\mathbf{x}) = \sum_{B=1}^{N_p} N_B(\mathbf{x}) u_{jB} & p^h(\mathbf{x}) &= \sum_{B=1}^{N_p} \tilde{N}_B(\mathbf{x}) p_B \\ \mathbf{v}^h(\mathbf{x}) &= \sum_{i=1}^N v_i^h(\mathbf{x}) \mathbf{e}_i \quad ; \quad v_i^h(\mathbf{x}) = \sum_{A=1}^{N_p} N_A(\mathbf{x}) v_{iA} & q^h(\mathbf{x}) &= \sum_{A=1}^{N_p} \tilde{N}_A(\mathbf{x}) q_A \end{aligned} \quad (6)$$

The finite element subspaces for velocity (\mathbf{V}^h) and pressure (P^h) being given by:

$$\begin{aligned} \mathbf{V}^h &= \{ \mathbf{v} \in H_0^1(\Omega)^N \mid \mathbf{v}_K \in R_k(K)^N, K \in \Omega^h \} \\ P^h &= \{ q \in C^0(\Omega) \cap L_0^2(\Omega) \mid q_K \in R_l(K), K \in \Omega^h \} \\ \mathbf{V}_g^h &= \{ \mathbf{v} \in H^1(\Omega)^N \mid \mathbf{v}_K \in R_k(K)^N, K \in \Omega^h, \mathbf{v} = \mathbf{u}_g \text{ on } \Gamma_g \} \end{aligned} \quad (7)$$

with $C^0(\Omega)$ representing the space of continuous functions, $L^2(\Omega)$ the Hilbert space of square integrable functions in Ω , $H^1(\Omega)$ the Sobolev functional space of functions with square integrable value and derivatives in Ω , R_k and R_l the polynomial of degrees k and l in Ω^h and N represents the number of space dimensions considered in the problem.

3.1. Galerkin Least-Squares formulation

The GLS formulation may be stated as: Find the pair $(u_i^h, p^h) \in V_{g_i}^h \times P^h, i=1, \dots, N$, such that:

$$B(u_i^h, p^h; v_i^h, q^h) = F(v_i^h, q^h), \quad \forall (v_i^h, q^h) \in V_i^h \times P^h \quad (8)$$

where

$$\begin{aligned} B(u_i^h, p^h; v_i^h, q^h) &= \int_{\Omega} \rho (u_j^h \partial_{x_j} u_i^h) v_i^h d\Omega + \int_{\Omega} 2\eta(\dot{\gamma}) D(u^h)_{ij} D(v^h)_{ij} d\Omega \\ &- \int_{\Omega} 2D(u^h)_{ij} \partial_{x_j} \eta(\dot{\gamma})^h \cdot v_i^h d\Omega - \int_{\Omega} p^h \partial_{x_i} v_i^h d\Omega - \int_{\Omega} \partial_{x_i} u_i^h q^h d\Omega + \epsilon \int_{\Omega} p^h q^h d\Omega \\ &+ \sum_{K \in \Omega^h} \int_{\Omega_K} (\rho (u_j^h \partial_{x_j} u_i^h) + \partial_{x_i} p^h - 2\eta(\dot{\gamma}) \partial_{x_j} D(u^h)_{ij} - 2D(u^h)_{ij} \partial_{x_j} \eta(\dot{\gamma})^h) \\ &\cdot \tau(\text{Re}_K) (\rho (u_j^h \partial_{x_j} v_i^h) - \partial_{x_i} q^h + 2\eta(\dot{\gamma}) \partial_{x_j} D(v^h)_{ij} + 2D(v^h)_{ij} \partial_{x_j} \eta(\dot{\gamma})^h) d\Omega \end{aligned} \quad (9)$$

and

$$\begin{aligned} F(\mathbf{v}, q) &= \int_{\Omega} \mathbf{f}_i v_i^h d\Omega + \int_{\Gamma} t_i v_i^h d\Omega \\ &+ \sum_{K \in \Omega^h} \int_{\Omega_K} \mathbf{f}_i \tau(\text{Re}_K) (\rho (u_j^h \partial_{x_j} v_i^h) - \partial_{x_i} q^h + 2\eta \partial_{x_j} D(v^h)_{ij} + 2D(v^h)_{ij} \partial_{x_j} \eta(\dot{\gamma})^h) d\Omega \end{aligned} \quad (10)$$

with ϵ denoting a positive constant $\epsilon \ll 1$ and $\tau(\text{Re}_K)$ the GLS stability parameter, defined as in Franca and Frey (1992):

$$\begin{aligned} \tau(\text{Re}_K) &= \frac{h_K}{2|\mathbf{u}|_p} \xi(\text{Re}_K) \quad \text{with} \quad \xi(\text{Re}_K) = \begin{cases} \text{Re}_K, & 0 < \text{Re}_K < 1 \\ 1, & \text{Re}_K > 1 \end{cases} \\ \text{Re}_K &= \frac{\rho m_k |\mathbf{u}|_p h_K}{4\eta(\dot{\gamma})} \quad \text{with} \quad m_k = \min\{1/3, 2C_k\} \\ \text{and } C_k &= \sum_{K \in \Omega^h} h_K^2 \|\text{div} \mathbf{D}(\mathbf{v}^h)\|_{0,K}^2 \geq \|\mathbf{D}(\mathbf{v}^h)\|_0^2 \quad \forall \mathbf{v}^h \in \mathbf{V}^h \end{aligned} \quad (11)$$

where h_K stands for the K -element size, Re_K is the grid Reynolds number $|\mathbf{u}|_p$ the p -norm on \mathbb{R}^N and the remaining variables have been defined as before.

The convergence proof is found in Franca and Frey (1992), based on a stability lemma, assuming the given data $\mathbf{a}(\mathbf{x})$ (a known velocity field) and $\eta(\mathbf{x})$ to satisfy $\text{div}(\mathbf{a}(\mathbf{x}))=0$ and $\eta=\text{constant}>0$, making $\mathbf{v}^h=\mathbf{u}^h$ and $q^h=-p^h$ and considering Eq. (9), the authors have achieved that:

$$B(\mathbf{u}^h, p^h; \mathbf{u}^h, -p^h) = \frac{1}{2} (2\eta \|\mathbf{D}(\mathbf{u}^h)\|_0^2 + \sum_{K \in \Omega^h} \|\tau^{1/2} ((\nabla \mathbf{u}^h) \mathbf{a} + \nabla p^h)\|_{0,K}^2) \quad (12)$$

3.2. Non linear strategy

Introducing the shape functions for $\mathbf{u}^h, p^h, \mathbf{v}^h$ and q^h (Eq. (6)) into the GLS formulation presented in Eqs. (8)-(11), the following residual form is obtained:

$$\mathbf{R}(\mathbf{U})=0 \quad (13)$$

where \mathbf{U} is the vector of degrees of freedom of \mathbf{u}^h and p^h and $\mathbf{R}(\mathbf{U})$ is given by:

$$\mathbf{R}(\mathbf{U}) = \mathbf{N}(\mathbf{u})\mathbf{u} + \mathbf{N}_\tau(\eta(\dot{\gamma}), \mathbf{u})\mathbf{u} + [\mathbf{K}(\eta(\dot{\gamma})) + \mathbf{K}_\tau(\eta(\dot{\gamma}), \mathbf{u})]\mathbf{u} + [\mathbf{G} + \mathbf{G}_\tau(\eta(\dot{\gamma}), \mathbf{u})]\mathbf{p} + \mathbf{G}^T\mathbf{u} - \mathbf{F} - \mathbf{F}_\tau(\eta(\dot{\gamma}), \mathbf{u}) \quad (14)$$

In Equation (14), matrices $[\mathbf{K}]$ and $[\mathbf{G}]$ are originated by the diffusive and pressure terms of Eqs.(8)-(10), respectively, with $\mathbf{N}(\mathbf{u})$, \mathbf{G}^T and \mathbf{F} , coming from the advective, incompressibility and body force ones, respectively. The least-squares terms of Eqs.(8)-(10) generate \mathbf{N}_τ , \mathbf{K}_τ , \mathbf{G}_τ and \mathbf{F}_τ . To solve the non linear matrix system presented in Eqs.(13)-(14) an incremental quasi-Newton method (see, for instance, Zinani and Frey, 2006) has been implemented where the Jacobian matrix, presented below, was updated only at each two or three iterations.

$$\mathbf{J}(\mathbf{U}) = \mathbf{N}(\mathbf{u}) + \frac{\partial \mathbf{N}(\mathbf{u})}{\partial \mathbf{u}}\mathbf{u} + \mathbf{N}_\tau(\eta(\dot{\gamma}), \mathbf{u}) + \frac{\partial \mathbf{N}_\tau(\eta(\dot{\gamma}), \mathbf{u})}{\partial \mathbf{u}}\mathbf{u} + \mathbf{K}(\eta(\dot{\gamma})) + \mathbf{K}_\tau(\eta(\dot{\gamma}), \mathbf{u}) + \frac{\partial \mathbf{K}_\tau(\eta(\dot{\gamma}), \mathbf{u})}{\partial \mathbf{u}}\mathbf{u} + \mathbf{G} + \mathbf{G}_\tau(\eta(\dot{\gamma}), \mathbf{u}) + \frac{\partial \mathbf{G}_\tau(\eta(\dot{\gamma}), \mathbf{u})}{\partial \mathbf{u}}\mathbf{p} + \mathbf{G}^T - \frac{\partial \mathbf{F}_\tau(\eta(\dot{\gamma}), \mathbf{u})}{\partial \mathbf{u}} \quad (15)$$

The algorithm below describes the numerical procedure:

ALGORITHM:

- I. Estimate vector \mathbf{U}^0 and set the number of iterations (m) to update Jacobian matrix $\mathbf{J}(\mathbf{U})$.
- II. Set $k=0, j=0, \epsilon=10^{-7}$.
- III. If $k - \text{int}(k/m) * k = 0$, then $j=k$.
- IV. Solve for incremental vector \mathbf{a}^{k+1} :

$$\mathbf{J}(\mathbf{U}^j)\mathbf{a}^{k+1} = -\mathbf{R}(\mathbf{U}^k) \quad (16)$$

where $\mathbf{R}(\mathbf{U})$ is given by Eq.(14) and $\mathbf{J}(\mathbf{U})$ is given by Eq.(15).

- V. Compute vector \mathbf{U}^{k+1} :

$$\mathbf{U}^{k+1} = \mathbf{U}^k + \mathbf{a}^{k+1} \quad (17)$$

- VI. If $|\mathbf{R}(\mathbf{U}^k)|_\infty > \epsilon$ then do $k=k+1$ and go step III; otherwise, store solution \mathbf{U}^{k+1} and exit from the algorithm.

4. NUMERICAL RESULTS

In order to compare results obtained by Galerkin and GLS methodologies, a bi-unity cavity with impermeability and no-slip boundary condition at its walls, except for the lid at the superior edge, which moves with a steady horizontal prescribed unitary velocity, was simulated for creeping flows of a Bingham fluid considering $\text{Bn}=3.9$.

Figure 1 represents the pressure at the centerline ($y=0.5$) and the horizontal velocity profile at the centerline ($x=0.5$) of the above described cavity, obtained by employing 10x10 and 100x100 Q1/Q1 element meshes considering both Galerkin and GLS methodologies. Concerning the Galerkin approximation, pressure oscillations still persist even refining the mesh, while velocity oscillations are substantially dampened with mesh refinement.

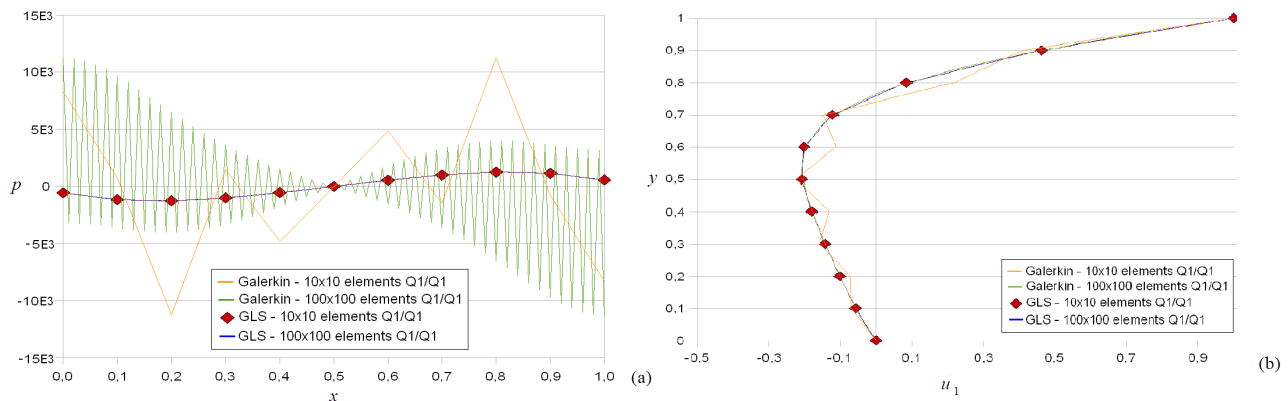


Figure 1: Galerkin and GLS approximations for (a) pressure plot at $y=0.5$; (b) horizontal velocity profile at $x=0.5$.

The numerical simulation, employing the GLS formulation defined by Eqs.(8)-(11), only considered half a planar symmetric abrupt expansion as described in Fig. 2. In order to achieve a Bingham fully-developed velocity profile upwind and downwind the expansion, the channel inlet and outlet had the lengths: $L_i=8H_i$, and $L_o=52H_i$. At channel

walls no-slip and impermeability were imposed and symmetry condition was considered at channel centerline. The channel aspect ratio was defined as $H_o/H_i=4$, the value of $H_i \equiv L$ has been set equal to 1, the plastic viscosity η_0 equal to 1. Bingham fully-developed profile, based on the equation deduced by Slattery (1999), was imposed at inlet and outlet:

$$u_1 = \frac{H_j^2 \nabla p}{2L_j \eta_0} \left[1 - \left(\frac{y}{H_j} \right)^2 \right] - \frac{\tau_0 H_j}{\eta_0} \left(1 - \frac{y}{H_j} \right) \quad \text{if } \frac{H_j \Delta p}{2L_j} \geq \tau_0$$

$$u_1 = 0 \quad (\text{plug flow}) \quad \text{if } \frac{H_j \Delta p}{2L_j} < \tau_0$$
(19)

with $j=i$ and $j=o$ denoting inlet and outlet, defined in Fig. 2, respectively and Δp the pressure difference.

All the computations have been performed with the finite element code for fluids under development at Laboratory of Computational and Applied Fluid Mechanics (LAMAC-UFRGS).

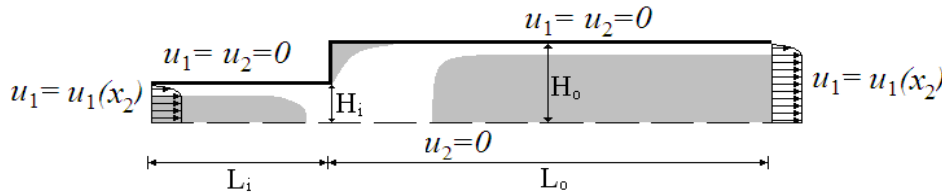


Figure 2: Problem statement.

After assuring mesh independence, by testing five different meshes, ranging from 6,920 to 29,980 Lagrangian bilinear finite elements (Q_1/Q_1) – as shown in Fig. 3, a mesh with 23,120 Lagrangian bilinear finite elements and 23,535 nodes has been selected, employing a criterion of 3% maximum allowed error between the dimensionless pressure drop of two consecutive meshes.

A detail of the adopted mesh to simulate a 4:1 planar expansion is presented in Fig. 3, showing the mesh refinement downstream and upstream the expansion, allowing to better characterize the yielded and unyielded surfaces in this region.

Throughout this article, the Papanastasiou regularization parameter m , was taken equal to 1000, as suggested by Mitsoulis and Huilgol (2004). Bingham and Reynolds numbers are defined as follows:

$$\text{Bn} = \frac{2\tau_0 H_i}{\eta_0 u_i} = \frac{2\tau_0 L}{\eta_0 u_i} \quad ; \quad \text{Re} = \frac{\rho u_i H_i}{\eta_0} = \frac{\rho u_i L}{\eta_0}$$
(20)

where variables are defined as before.

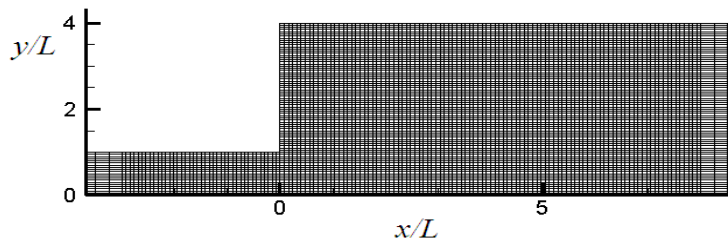


Figure 3: Detail of the employed mesh for a 4:1 planar expansion.

In Figure 4 the yielded and unyielded zones (represented by the black regions) were depicted for inertialess flows with Bingham number ranging from $\text{Bn}=0.2$ to $\text{Bn}=127$. The unyielded regions can be sorted in two distinct zones: unmoving rigid zones, or simply dead zones, at expansion corners, and moving rigid zones (plug flows) on channel centerline. As Bn increases the unyielded zones – dead zones at the expansion corners and plug flow zones in both channels – also increase. In Fig 4(a), for $\text{Bn}=0.2$, a very small plug flow is observed upstream the contraction, while the plug flow occupies almost its whole domain for $\text{Bn}=127$ (Fig. 4(d)). Also for very small Bn ($\text{Bn}=0.2$) the downstream rigid moving zone is pushed away from the expansion corner – when compared with Figures 4(b)-4(d). Actually, the plug flow begins almost at the same distance from the corner in these later figures. The effect of increasing Bn downstream the corner is enlarging the plug flow zone. In short, dead zones and plug flows increase with the growth of Bingham number.

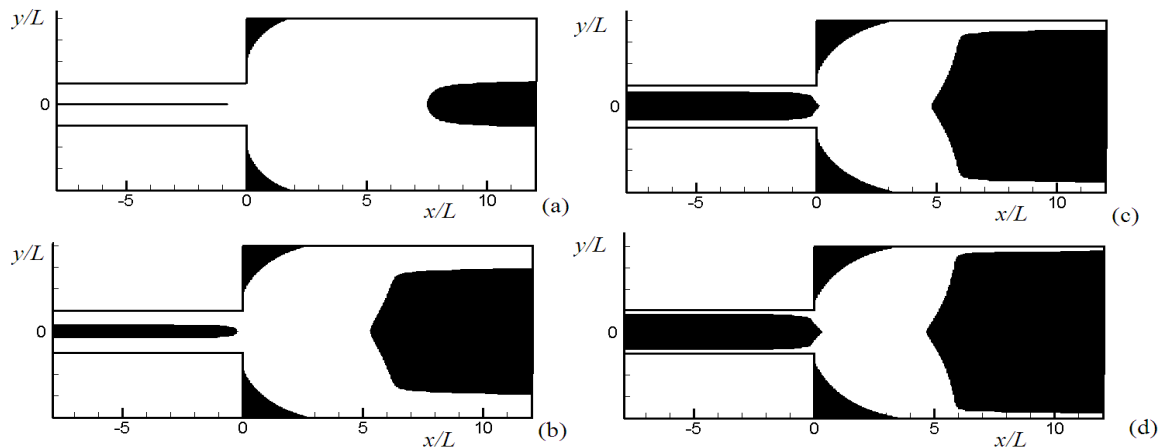


Figure 4: Yielded and unyielded regions for $Re=0$ and (a) $Bn=0.2$, (b) $Bn=3.9$, (c) $Bn=27.1$, (d) $Bn=127$.

A 2:1 abrupt expansion has been simulated in this work in order to compare the results with those by Mitsoulis and Huigol (2004), for two distinct values of Bingham number – namely $Bn=27.1$ and $Bn=127$, as presented in Fig. 5. The yield surfaces – limiting surfaces between yielded and unyielded zones – presented an acceptable agreement.

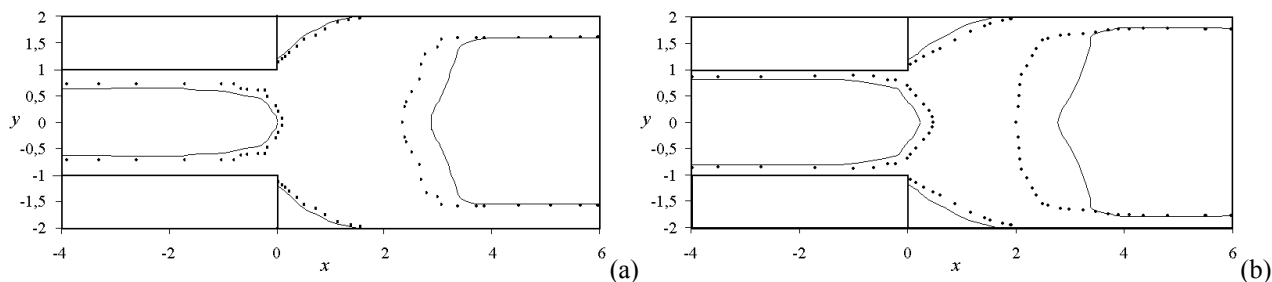


Figure 5: Comparison of results for an aspect ratio $H_0/H_f=2$ obtained in the present work with those by Mitsoulis and Huigol (2004): (a) $Bn=27.1$; (b) $Bn=127$.

Figure 6 depicts the influence of the Bingham number on dead zone length and distance from expansion to rigid moving zone, considering the regularizing parameter $m=1000$ and $Re=0$. As Bn increases, both dead zones and plug flow regions grow too.

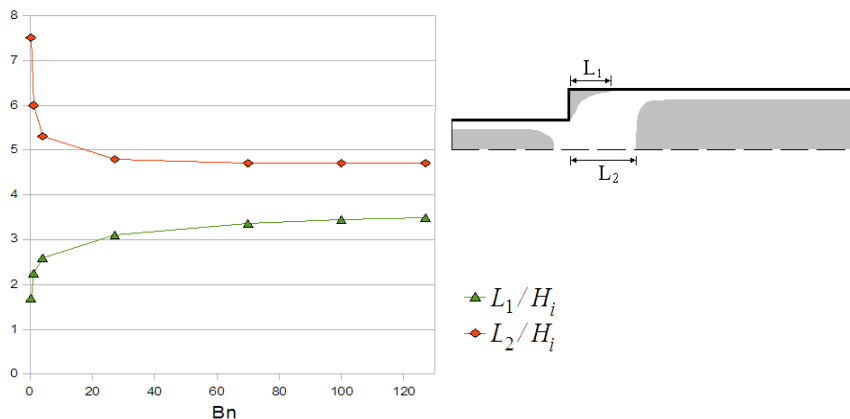


Figure 6: Influence of the Bingham number. Dead zone length and distance from expansion to rigid moving zone, for $m=1000$ and $Re=0$.

Figure 7 illustrates the influence of the Bingham number on horizontal velocity profile at a fully developed region of the larger channel and the pressure drop through the channel, considering $m=1000$ and $Re=0$. As the Bingham

number grows, the velocity profiles become flatter and subjected to severe boundary layers (plug-flows) with higher shear rates, and the pressure drop through the channel is highly increased.

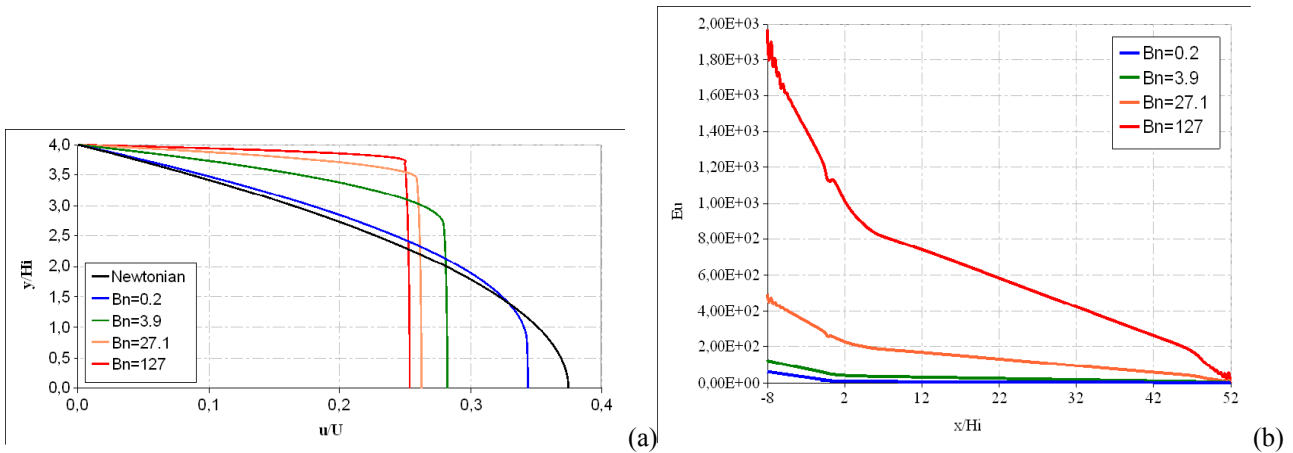


Figure 7: Influence of the Bingham number for $m=1000$ and $Re=0$. (a) Horizontal velocity profile at a fully developed region of the larger channel; (b) Pressure drop through the channel.

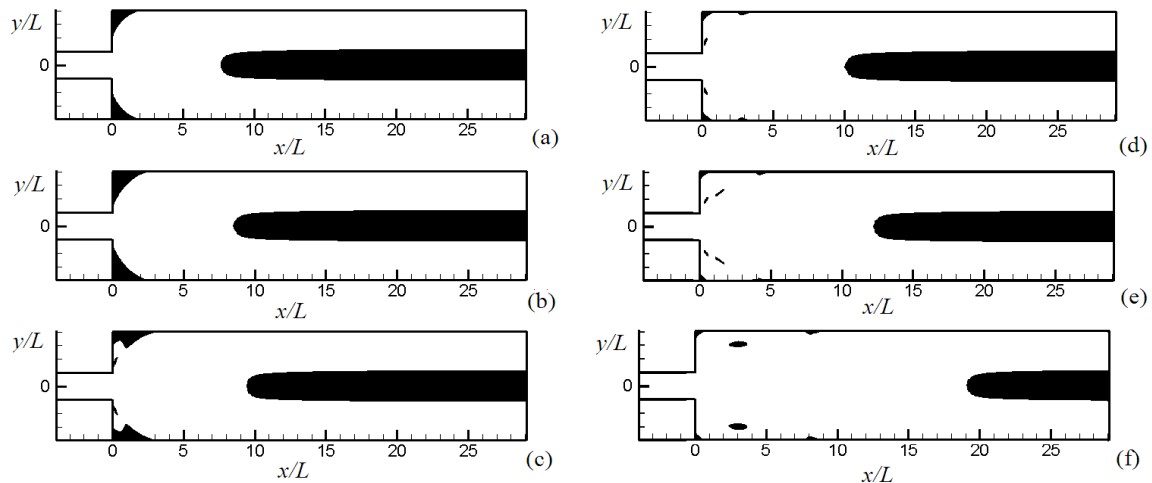


Figure 8: Influence of Reynolds number at yielded and unyielded regions for $Bn=0.2$, $m=1000$ and (a) $Re=1$; (b) $Re=5$; (c) $Re=8$; (d) $Re=10$; (e) $Re=13$; (f) $Re=30$.

In Figure 8, in order to investigate the influence of Reynolds number, a very low Bingham number was chosen – namely $Bn=0.2$ – with the regularization parameter $m=1000$. Initially, as Re has been increased the unyielded dead zones have been increased too – as shown in Figs. 8(a-f). However, after a critical value around $Re=8$, this growth experimented a reverse behavior, probably due to the collapse of the dead zone – Figs. 8(c) to 8(f). Also the downstream unyielded moving zones were clearly pushed away from the expansion corner as Re was increased.

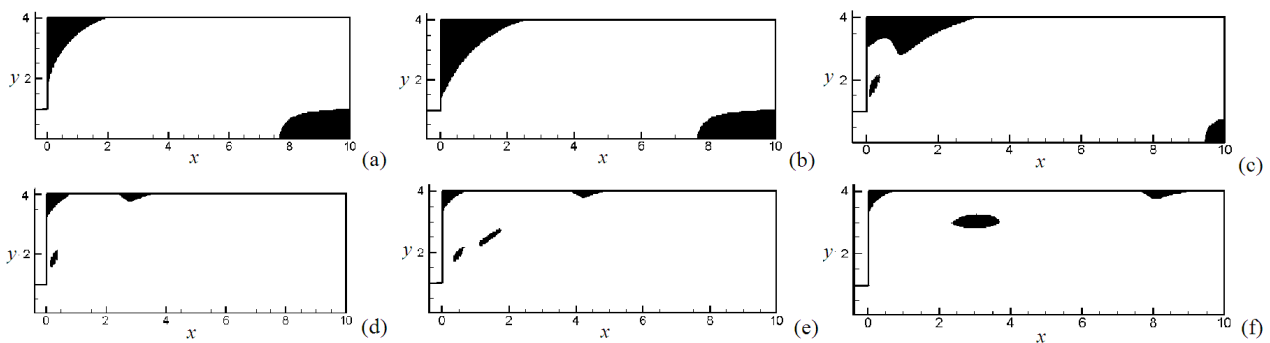


Figure 9: Influence of Reynolds number at expansion corner region for $Bn=0.2$, $m=1000$ and (a) $Re=1$; (b) $Re=5$; (c) $Re=8$; (d) $Re=10$; (e) $Re=13$; (f) $Re=30$.

Figure 9 describes the influence of Reynolds number at expansion corner region, once again for $m = 1000$ and $Bn = 0.2$, ranging the Reynolds number from 1 to 30. Here may be better observed that, near $Re \approx 8$, the dead zone starts to break up and detaches from the expansion corner. This effect has already been experimentally observed for the axisymmetric flow obtained by Jay et al. (2001), depicted in Fig. 10.

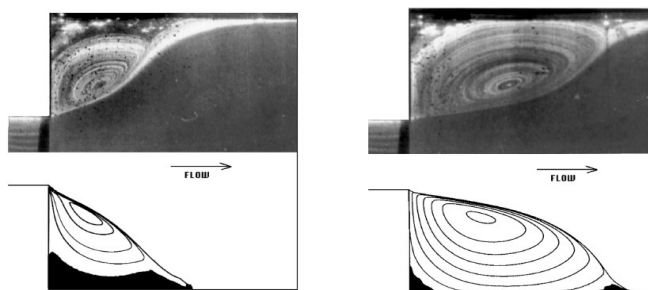


Figure 10: Experimental results for axisymmetric shear-thinning viscoplastic flow (Jay et al., 2001).

5. FINAL REMARKS

A Galerkin least-squares finite element formulation has been employed to approximate a 4:1 sudden expansion flow of Bingham fluids, in which the regularized Bingham model was employed. The numerical methodology has stably approximated linear viscoplastic flows, even for a combination of subspaces for velocity and pressure violating the Babuska-Brezzi condition. As it might be expected, for equal-order interpolations Q1/Q1, the classical Galerkin method has generated unstable approximations even for simulations employing refined meshes. For creeping flows, unyielded zones were greater for fluids with higher yield stress. The more viscoplastic the material, the higher pressure drops, due to the growth of plug-flows and dead zones. Besides, the growth of the unyielded zones with the Bingham number and an inflexion in dependence of the growth of the dead zone at expansion corner with the Reynolds number were verified.

6. ACKNOWLEDGEMENTS

The author F. Silveira thanks for its undergraduate scholarship provided by FAPERGS. Author S. Frey acknowledges CNPq and author M. L. Martins-Costa acknowledges CNPq and FAPERJ, for financial support and grants.

7. REFERENCES

- Bird, R. B., Dai, G. C., 1983, "The Rheology and flow of viscoplastic materials". Freund Publishing House, U.S.A.
- Babuška I., 1973. "The finite element method with lagrangean multipliers". vol. 20, pp.179-192.
- Brezzi F., 1974. "On the existence, uniqueness and approximation of saddle-point problems arising from Lagrange multipliers", RAIRO Anal. Numér., vol. 8, pp. 129-151.
- Franca, L.P., and Frey, S., 1992, "Stabilized finite element methods: II. The incompressible Navier-Stokes equations", Comput. Methods Appl. Mech. Engrg., v. 99, pp. 209-233.
- Jay, P., Magnin, A. and Piau, J.M., 2001, "Viscoplastic fluid flow through a sudden axisymmetric expansion", AIChE Journal, v. 47, No. 10, pp. 2155-2166.
- Mitsoulis, E., Huilgol, R.R, 2004, "Entry flows of Bingham plastics in expansions", J. Non-Newtonian Fluid Mech., v. 122, pp. 45-54.
- Papanastasiou, T.C., 1987, "Flows of materials with yield", J. Rheology, v. 31, pp. 385-404.
- Slattery, J. C., 1999, "Advanced Transport Phenomena", Cambridge University Press, U.S.A.
- Zinani, F., Frey, S., 2006, "Galerkin Least-Squares Finite Element Approximations for Isochoric Flows of Viscoplastic Liquids", Journal of Fluids Engineering – Transactions of the ASME, Vol. 128, pp. 853-863.

8. RESPONSIBILITY NOTICE

The authors are the only responsible for the printed material included in this paper.